

Element technologies of fixed-abrasive tools with a spiral wire used for high-precision machining

Y. Kamimura¹, K. Tsuchiya¹

¹ *Institute of Industrial Science, University of Tokyo, Japan*

kamimura@iis.u-tokyo.ac.jp

Abstract

Damage (latent flaws) on the surface of SiC single crystals caused by scratches during their high-precision processing is a problem [1]. The main cause of such scratches is the variation in the diameter of abrasive grains used in mechanical polishing. The aim of this study is to use fixed-abrasive tools with a spiral wire, instead of conventional mechanical polishing tools. We developed a tool with continuous pores, i.e., spiral channels [2], used as the chip pockets to prevent the loading of the pores with swarf. Here, the falling off of abrasive grains is prevented by electroplating. To reduce the nonuniform depth of cut caused by the variation of abrasive grains, the tool run-out associated with the revolution of the tool and the fluctuation in the processing pressure depending on the tool shape are suppressed. The results indicate that (1) filling the abrasive-grain layer with a resin can decrease the actual surface roughness obtained using the tool compared with the theoretical roughness of the finished surface owing to the dispersion effect of the processing pressure, leading to the suppression of the effects of tool run-out, and (2) by making the tool strawberry-shaped, the fluctuation in the processing pressure is decreased and the depth of cut, used as an indicator of surface roughness, becomes stable, thereby realized a high-precision machining of pure aluminum ($R_a=7.8\text{nm}$) using the variation of $\phi 5\text{-}\phi 12\mu\text{m}$ diamond grains.

1. Effect of resin-filled tool

In general, the pores (chip pockets) of grinding tools are indispensable as one of the three elements of grinding wheels. With the developed spiral tool, a spiral channel is formed between the adjacent turns of the spirally wound thin wire and positioned close to the abrasive-grain layer [Fig. 1(b)]. Continuous discharge of swarf is possible using the spiral channel as the chip pocket. Loading can be prevented with this spiral structure; however, the roughness of the surface processed using the tool is

approximately $R_a=30\text{nm}$. The reasons for this high R_a are the vibration of the tool upon contact with the workpiece (tool run-out), the variation of abrasive grains, and the fluctuation in the processing pressure. The tool run-out is mainly caused by the vibration of the tool associated with its high-speed revolution. As a countermeasure against tool run-out, the filling of resin in the abrasive-grain layer is examined. Figure 2 shows the concept of the filling. Tool run-out (a) is calculated by dividing the processing pressure applied to the tool (grinding force, F_n) by the area of the tool that is in contact with the workpiece S_n , i.e., $a=F_n/S_n$. The processing pressure is constant for both resin-filled and unfilled tools. As is obvious from the equation, S_n of the resin-filled tool (b) is larger than that of the unfilled tool (a). Therefore, the grinding force is more dispersed for the resin-filled tool. With this dispersion effect, the tool run-out of the resin-filled tool (a_2) is smaller than that of the unfilled tool (a_1), suppressing the amount of run-out and improving the surface roughness.

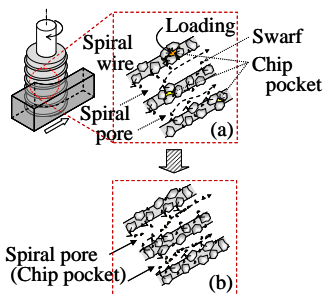


Figure 1: Chip pocket of spiral tool

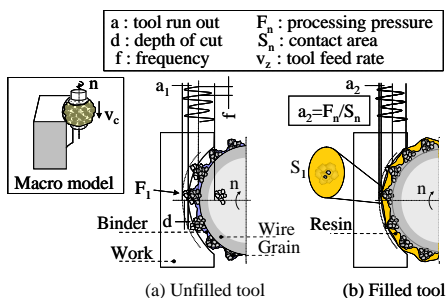


Figure 2: Concept of resin-filled tool

2. Resin-filled tool

2.1 Comparison of roughness used resin-filled and unfilled tool

Table 1 shows the specifications of the resin-filled tool. Nonconductive diamond abrasive grains ($\phi 20\text{-}30\mu\text{m}$) are used as the abrasive grains, and water-soluble fluorinated resin is used as the filling material. The workpiece was pure aluminum (A1050), which easily causes loading, and processed to form a semicylinder shape as shown in Fig. 3. Figure 4 shows the roughness of the surfaces obtained by grinding using the unfilled and resin-filled tools with respect to the revolution. The surface roughness of approximately $R_a=18\text{nm}$ was obtained at approximately 12000rpm for both tools. With decreasing revolution, the roughness of the surface obtained by grinding using the resin-filled tool improves, whereas that in the case of the unfilled

tool deteriorates. When the feed rate is constant, the feed pitch per tool revolution increases with decreasing revolution. Also the depth of cut is unstable because of the variation of abrasive grains and the surface roughness does not improve. The equation of the theoretical roughness of the finished surface is also applicable to the resin-filled tool. However, the actual roughness of the surface obtained with the resin-filled tool improves to approximately $R_a=12\text{nm}$, unlike that in the case of the unfilled tool. The reason for this is the dispersion of the processing pressure during grinding [Fig. 2(b)].

Table 1: Specifications of resin-filled tool

Substrate and wire	$\phi 10$ -SUS $\phi 0.4\text{mm}$ -copper	Grains 2g/0.3L	Diamond $\phi 20\text{-}30\mu\text{m}$
Spiral α	4degree		Ni coated dia $\phi 5\text{-}12\mu\text{m}$
Resin	Water-soluble resin	Tool ($\phi 10$)	Strawberry geometry (Curvature radius 10mm)
Workpiece	Pure aluminum		Columnar form
Feed V_z	$5\mu\text{m}/\text{sec}$	Depth of cut C_x	$5\mu\text{m}$

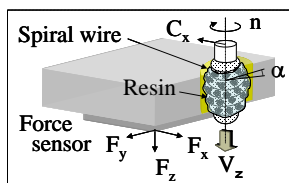


Figure 3: Processing method

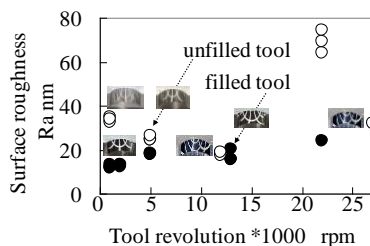


Figure 4: Comparison of roughness

2.2 Difference in processing pressure for different tool shapes

The diameter of the abrasive grains was further decreased to improve the surface roughness. Conductive diamond abrasive grains ($\phi 5\text{-}12\mu\text{m}$) coated with Ni were used to increase the ease of filling. Tools of two shapes, strawberry-shaped and columnar tools, were used to change the processing pressure during grinding. Figure 5 shows the photographs of the surfaces and the roughnesses of the surfaces obtained using strawberry-shaped and columnar tools. Both are resin-filled tools, and their revolution was set constant at 1000rpm. Although the workpiece has a mirror surface, the surface obtained with the columnar tool has a poor roughness of $R_a=45\text{nm}$. In contrast, the surface obtained with the strawberry-shaped tool has a high-quality

mirror finish and a roughness of $R_a=7.8\text{nm}$. Here, the grinding forces of the two tools were measured. For the strawberry-shaped tool, the grinding force and its variation for F_x and F_y are small regardless of the tool position (Fig. 6). In contrast, for the columnar tool, the grinding force F_x and its variation change significantly (Fig. 7) depending on the tool position. The variation in the grinding force leads to an unstable depth of cut. The processing pressure of the strawberry-shaped tool is more stable than that of the columnar tool, and a higher precision surface is obtained because the strawberry-shaped tool at its largest diameter is in constant contact with the workpiece. Therefore, the strawberry-shaped tool with an abrasive-grain layer filled with resin enables the dispersion of the processing pressure and the suppression of the fluctuation in the processing pressure, whereby the reduction of effects of the variation of abrasive grains can be expected.



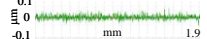
Filled tool, $\phi 5\text{-}12\mu\text{m}$ (Ni coated dia), 1000rpm, $V_s 5\mu\text{m/s}$, $C_s 5\mu\text{m}$		
Geometry	Surface	Roughness μm
Columnar		Ra 0.045 Rt 0.294
Strawberry		Ra 0.008 Rt 0.079
		

Figure 5: Comparison by geometry

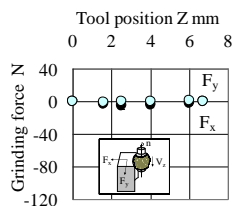


Figure 6: Strawberry

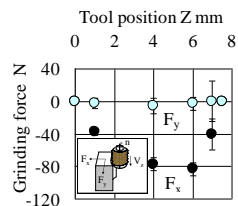


Figure 7: Columnar

3. Conclusions

- (1) By dispersing the processing pressure and minimizing the fluctuation in the processing pressure, the effects of the tool run-out were found to be suppressed. High-precision processing ($R_a = 7.8 \text{ nm}$) of pure aluminum was realized in this study using conductive abrasive grains ($5\text{-}12 \mu\text{m}$ in diameter).
- (2) The important factors in realizing high-precision processing using the developed spiral tools are the dispersion of the processing pressure and the suppression of the fluctuation in the processing pressure.

References:

[1] K. Abe. *JSAT*, Vol. 56/9, (2012), pp. 588-591.
 [2] Y. Kamimura, K. Tsuchiya, Y. Tani, S. Lee. Proc. of 12th, *euspen*, 6, (2012), pp. 241-245.